PSFC/JA-09-39

Experimental Studies of Edge Turbulence and Confinement in Alcator C-Mod

Cziegler, I., Terry, J. L., Hughes, J. W., LaBombard, B.

December 2009

Plasma Science and Fusion Center
Massachusetts Institute of Technology
Cambridge MA 02139 USA

This work was supported by the U.S. Department of Energy, Grant No. DE-FC02-99ER54512.

Experimental Studies of Edge Turbulence and Confinement in Alcator C-Mod

I. Cziegler,* J. L. Terry, J. W. Hughes, and B. LaBombard

Massachusetts Institute of Technology,

Plasma Science and Fusion Center,

167 Albany Street, Cambridge, MA, 02138

(Dated: January 14, 2010)

Abstract

The steep gradient edge region and Scrape-Off-Layer on the low-field-side of Alcator C-Mod (I.H. Hutchinson et al., Phys. Plasmas **1**, 1511 (1994)) tokamak plasmas are studied using gas-puff-imaging diagnostics. In L-mode plasmas, the region extending $\sim$ 2cm inside the magnetic separatrix has fluctuations showing a broad, turbulent spectrum, propagating in the electron diamagnetic drift direction, whereas features in the open field line region propagate in the ion diamagnetic drift direction. This structure is robust against toroidal field strength, poloidal null-point geometry, plasma current and plasma density. Global parameter dependence of spectral and spatial structure of the turbulence inside the separatrix is explored and characterized, and both the intensity and spectral distributions are found to depend strongly on the plasma density normalized to the tokamak density limit. In H-mode discharges the fluctuations at and inside the magnetic separatrix show fundamentally different trends compared to L-mode, with the electron diamagnetic direction propagating turbulence greatly reduced in ELM-free, and completely dominated by the mode-like structure of the Quasi-Coherent Mode in Enhanced D-Alpha regimes (A.E. Hubbard et al., Phys. Plasmas **8**, 2033 (2001)), while the normalized SOL turbulence is largely unaffected.

*cziegler@psfc.mit.edu

I. INTRODUCTION

The region at the edge of tokamak plasmas exhibiting a steep gradient in plasma density and temperature in the low confinement regime (L-mode) and a density- and temperature-pedestal in the high confinement regime (H-mode) is crucial for the understanding of confinement states, transport and plasma–wall interactions. Cross-field transport across the last closed flux surface (LCFS) and the near Scrape-Off-Layer (SOL) is believed to be directly linked with the global confinement properties of the plasma [1–4], as well as the physics of the L-H transition itself. In the open field line region, particle transport is found to be dominated by intermittent events – radially propagating plasma "blobs"– in nearly all types of magnetically confined plasmas [5, 6, 8–11]; and although recent experimental studies on low pressure devices [12] have linked the formation mechanism of these structures to theoretically expected instabilities, blob-generation in tokamaks is still not well understood.

Nevertheless, recent experiments on Alcator C-Mod [13] have revealed a number of connections between global operating parameters (density and temperature profiles, plasma currents) and dimensionless scaling parameters of electromagnetic turbulence. These advances, together with the above transport phenomenology have led to the hypothesis that edge transport physics is described as a system near marginal stability [14, 15]. Therefore, both electromagnetic instabilities and critical gradients are of interest since they are thought to play a decisive role inside the LCFS determining the width of the edge gradient in all confinement regimes. Moreover, in the low-field-side pedestal, decidedly mode-like plasma responses, such as the Quasi-Coherent Mode of the Enhanced D-Alpha (EDA) H-mode [16] are found, which are known to drive particle transport [17]. How these modes develop and what their connection is to edge turbulence remains a question.

Finally, all the above dynamics and their dependence on plasma density (or collisionality) are thought to play an essential role in the physics that sets the robust Greenwald density limit [18]. With that as motivation we describe the dependence of the edge turbulence characteristics upon electron density normalized to the Greenwald density.

This paper reports a set of recent experimental observations of edge turbulence structure in a radially broad zone at high time resolution at the low-field-side of Alcator C-Mod and its connections and implications to particle transport. Section II describes the main diagnostics and the region observed in this study. Measurements of edge and SOL turbulence spectra,

propagation velocities and their trends in both L-mode and H-mode discharges are presented in Section III. First the general findings from L-mode plasmas are introduced, which also provides some background for the H-mode experiments and motivation for concentrating on the turbulence of the edge region. In particular, the edge turbulence is shown to respond quite sensitively to plasma density. Then results from H-mode experiments are used to present further evidence for the connection of edge turbulence (ie turbulence just inside the LCFS) and cross-field particle transport, by showing that the different confinement regimes have specific "fingerprints" in the dispersion relations of the observed turbulence. Since the two subsections treat different kinds of plasma discharges, their descriptions are included at the beginning of each subsection. Finally, Section IV summarizes the major findings, relates them to the trends found in the SOL, and makes an attempt at outlining a picture of the edge/SOL region.

II. EXPERIMENTAL SETUP

A poloidal section of Alcator C-Mod is shown in Fig. 1 with cross sections of the magnetic flux surfaces of a typical lower-single-null (LSN) equilibrium and the schematic of the array of gas-puff-imaging (GPI) diagnostic views overlaid. The diagnostic focuses on the low-field-side "midplane" region using a 9×10 array of in-vessel optical fibers with toroidally viewing, horizontal lines of sight. The optics are filtered to receive the deuterium Balmer α line ($\lambda = 656$nm) which is locally enhanced at the toroidal position of the system's focus by a D_2 gas puff from a nearby nozzle. The fibers are coupled to high sensitivity (quantum efficiency at 656nm = 0.8) avalanche-photo-diodes (APD). The APD's and their electronics are cooled to 15°C in order to maximize the Signal-to-Noise-Ratio and maintain a constant APD gain (typically ~ 50). The bandwidth of the electronics is $BW \gtrsim 1$MHz, and the signals are digitized at a rate of 2M frames per second. Due to the low noise characteristics of the detectors and amplifiers, the system is photon noise limited above 500kHz at the light intensities commonly encountered.

The viewing area is 4cm (radial)$\times$4.4cm (vertical), with an in-focus spot size of 3.7mm for each of the 90 individual channels, viewing the region with major radii of 88cm $< R <$ 92cm and heights-above-axis of -5.4cm $< z < -1$cm. Note that the radial extent of the field of view $L_{vis} = 4$cm ($\approx 0.2\times$ minor radius) is broad compared to the relevant physical size

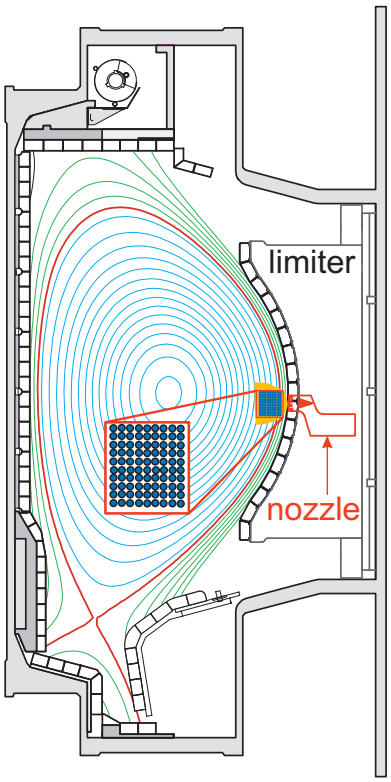

FIG. 1. (color online) The cross section of Alcator C-Mod with a representative LSN magnetic equilibrium. The diagnostic gas puff enters from a nozzle mounted in the low-field-side limiter, 2.54 cm below the height of the magnetic axis. The 2D GPI viewing array covers 4cm × 4.4cm at this location, extending both into the region of closed flux surfaces (blue) and open field lines (green).

scales of the plasma edge: the characteristic length of the pressure profile, $L_{vis} \gtrsim 6L_p$ and the sound gyro-radius $L_{vis} \gtrsim 60\rho_s$.

In this paper we report the observation of clear differences in the turbulence characteristics of the open and closed flux surface regions, consequently we distinguish between the regions by using the term *"edge" to refer exclusively to the* $\sim 2cm$ *wide region inside the last closed flux surface, as opposed to the "Scrape-Off-Layer" which is the region with open field lines.* Plots are often labeled by the ρ parameter, which in this form (without any indices) stands for the distance into the SOL as mapped to the height of the midplane on the low-field-side. The vertical columns of the viewing array are nearly aligned with the poloidal sections of the flux surfaces, so that the variation of ρ along a single vertical column is less than 1.5mm. Spatial Fourier-transforms along these columns therefore generate poloidal wavenumber information.

The excitation of the neutral gas depends on the number and average energy of electron-neutral collisions making the diagnostic sensitive to a combination of $\tilde{n_e}$ and $\tilde{T_e}$ [19]. The velocities measured from a spatial and temporal spectrum are therefore phase velocities of emission features.

In order to compare the motion of observed emission features with expected fluid motion and particle drifts, electron diamagnetic drift velocities in the edge and near SOL are estimated using n_e and T_e profiles from Thomson scattering [20], while radial electric field profiles in the SOL are evaluated from direct electric potential measurements made using scanning Langmuir probes.

III. OBSERVATIONS

A. L-mode

The structure and behavior of edge and SOL turbulence has been studied for a wide range of plasma parameters. Here we focus on LSN Ohmic L-mode discharges with I_p parallel to B_T and $\mathbf{B} \times \nabla \mathbf{B}$ towards the active X-point. Comparison between the general turbulence trends of LSN and USN discharges from the campaign of 2006-2007 showed very little differences, therefore we make no further reference to USN plasmas in this paper. Magnetic equilibria were set up for a range of plasma currents $0.4\text{MA} < I_p < 1.0\text{MA}$, and toroidal magnetic fields $2.6\text{T} < B_T < 6.8\text{T}$. Line averaged density $-\bar{n}_e-$ scans were performed at various combinations for $0.15 < \bar{n}_e/n_G < 0.45$, where $n_G(10^{20}\text{m}^{-3}) = I_p(\text{MA})/(\pi a^2(\text{m}^2))$ is the Greenwald-limit [21]. For the majority of discharges the safety factor at 95% of the flux was held constant at $q_{95} \approx 5$ but in the graphs showing collections of data from the scans, fixed B_T and scanned I_p data are included as well in order to separate out any potential current-related effects.

The radial profiles of the edge turbulence produced in all L-mode discharges are qualitatively the same. Both the edge and the SOL spectra are broad-band, yet there are clear differences between the two regions. The fluctuation levels relative to the average brightness levels of the views are significantly (about an order of magnitude) higher in the SOL than in the edge. Additionally, SOL emission signals are intermittent and produce distinctly different spectral distributions from those of the edge. Emission features of the edge show no

radial propagation, but pick up radial speed quickly once they cross the separatrix.

We have also characterized these regions by generating spatial as well as temporal Fourier transforms from the light signals. This yields 2-dimensional, wavenumber–frequency spectra $S(k_{pol}, f)$ from every vertical column in the array, ie 9 radial locations, spanning the edge and the SOL. Since typical turbulence spectra fall off rather rapidly with both k_{pol} and frequency, we normalize the spectra to every frequency band, as

$$S(k_{pol}|f) = \frac{S(k_{pol}, f)}{S(f)}$$

basically treating the spectrum as a probability distribution and generating the $S(k_{pol}|f)$ *conditional spectrum*, in order to highlight trends in the relatively high frequency, high wavenumber domain. Conditional spectra of L-modes show a characteristic radial profile (Fig. 2), in which fluctuations of the SOL produce a single lobe in the observed k_{pol}-f spectra with $k_{pol} < 0\text{cm}^{-1}$. A negative wavenumber in our sign convention means that the propagation is vertically *down*, in the *ion diamagnetic drift direction*. Edge turbulence, by contrast, is found to be dominated by $k_{pol} > 0\text{cm}^{-1}$ fluctuations, ie propagating in the *electron diamagnetic drift direction*. The measured k_{pol}-f spectra are well fitted by a linear dispersion relation up to high frequencies so that $v_{ph} = v_g$ for a broad range, and these velocities can be determined for every radial location (Fig. 3).

This propagation velocity trend across the separatrix may not be surprising. Given that parallel electron losses dominate on open field lines the radial electric field E_r of the SOL is positive, in accordance with $\phi_{\text{float}} \approx 3T_e/e$ (as in [22]) , setting the $\mathbf{E}\times\mathbf{B}$ direction parallel to what we labeled "ion diamagnetic drift direction" (IDD), additionally, previous GPI studies of the SOL have already shown a similar bulk propagation trend. In the edge, on the other hand, ion losses dominate due to neoclassical effects, rendering $E_r < 0$ in this zone, and generating an $\mathbf{E}\times\mathbf{B}$ drift in what we called the "electron diamagnetic drift direction" (EDD). However, there are details of the radial profiles that suggest a more subtle view.

Wavenumber-frequency spectra from the separatrix region, as in the middle graph in Fig. 2, show two counter-propagating lobes, with velocities very closely matching those found in the regions where the respective features dominate. The velocities are never found to transition smoothly from one direction to the other, rather, their velocities are remarkably constant with R; and in some cases the IDD propagating features exist as deep as $\rho = -1.7$cm in the plasma, albeit with low intensities. Figure 3 clearly demonstrates the velocity trend.

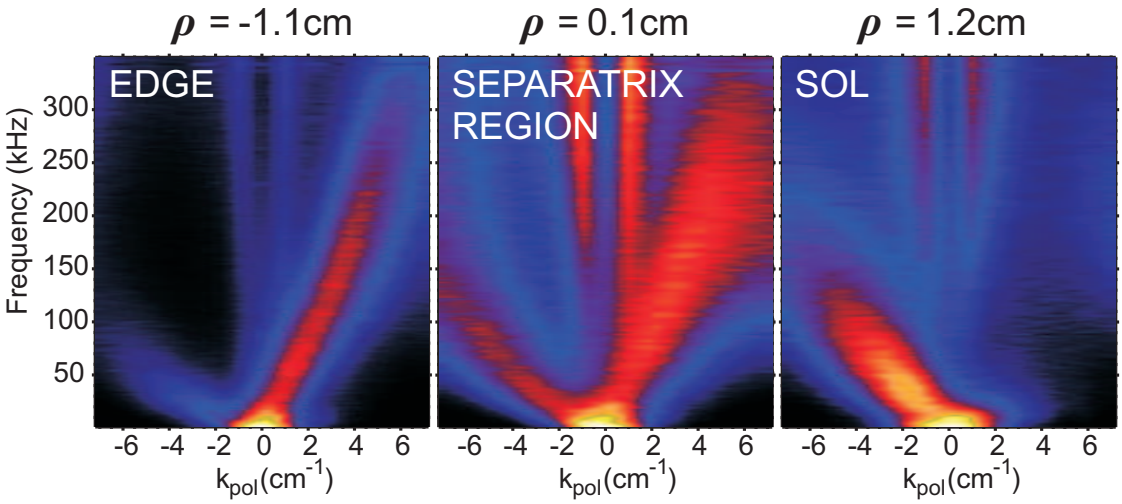

FIG. 2. (color online) Radial profile of the turbulence in poloidal wavenumber and frequency space. $k_{pol} > 0$ corresponds to propagation vertically up, in the EDD (see text) – this is characteristic in the edge, and $k_{pol} < 0$ to motion in the IDD, this is characteristic of the SOL. The middle graph shows the separatrix region in which instead of a slowly propagating feature, both features are seen with their well defined speeds. The two narrow spikes in the middle are caused by noise. $B_T = 5.4$T, $I_p = 0.8$MA, $\bar{n_e}/n_G = 0.45$

For comparison, we also plotted $v_E = E_r/B_T$ as a solid band (green), the thickness of which shows the error estimated from probe measurements. The probe measurement is made in a different discharge with similar q_{95} and Greenwald fraction ($I_p = 0.8$MA, $B_T = 5.4$T), since probe data were not available for the discharge plotted. In the far SOL, there is good agreement between v_E and the propagation velocities, but they manifestly deviate at $\rho \lesssim 0.5$cm. If the measured velocities were simply interpreted as $\mathbf{E} \times \mathbf{B}$ drifts, E_r would have to change sign in less than the 3.7mm spot size, and attain its maximal values. This is in disagreement with both previous probe results [13] and measurements of the radial electric field by charge-exchange recombination spectroscopy [23]. Interpretation of the *edge* propagation velocity solely as v_E in these regimes also contradicts the existence of the E_r-well found in ref. [23], which should cause a shear in the region where the edge turbulence propagation velocities seem to be largely invariant. The EDD velocities in the edge are close to the diamagnetic drift velocity $v_D = \nabla p_e/n_e e B_T$ also plotted in Fig. 3 as a solid (purple) curve, running below the measured phase velocities as expected, since v_E and v_D are in the same direction in the region.

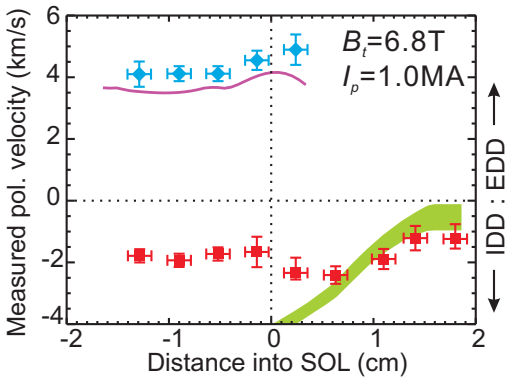

FIG. 3. Radial profile of the poloidal propagation velocities. Diamonds show the measured phase velocities of the positive k_{pol}, while squares show those for negative k_{pol}. The purple curve is the electron diamagnetic drift velocity profile and the green curve is the $\mathbf{E} \times \mathbf{B}$ velocity for $\rho > 0$.

The above observations suggest that the velocities measured belong to two distinct objects, a wavelike set of fluctuations dominant in the edge and plasma blobs moving generally with $\mathbf{E} \times \mathbf{B}$ in the SOL. This motivates treating the two lobes of the k_{pol}-f spectra separately even in the regions of overlap, and may have implications as to the generation mechanism of the SOL features from edge turbulence, to which we return in Sec. IV. Summing up the power of the two sides of the spectra separately yields Fig. 4 where we plotted the intensity profiles of both sides normalized to a sum of unity, so the regions of dominance may become apparent. The peak intensity (normalized to DC) of the SOL turbulence in the higher Greenwald fraction ($F_{Gr} = \bar{n}_e/n_G$) cases shifts outwards.

The *edge* turbulence spectra for positive k_{pol} plotted in Figure 5 show a number of remarkable features. Qualitatively, spectra scale with the Greenwald fraction: a high value of $\bar{n}_e/n_G$ gives a higher relative fluctuation level in the edge plasma. Figure 6 gives a more quantitative view on this scaling, showing the total relative fluctuation level above 50kHz from the positive k_{pol} side of spectra. The lower limit on the integration is chosen so as to exclude any contamination from the negative k_{pol} side, due to finite resolution.

The result shows a sensitive dependence of the turbulence power on Greenwald fraction, with a sharp increase in power around $\bar{n}_e/n_G = 0.25$ making a strong connection to ref. [13] and [14] where the density profile of the SOL was found to systematically flatten and its average density to increase as the line averaged density of the main plasma, and consequently F_{Gr} increased. This provides further evidence to the claim in the above references that n_G

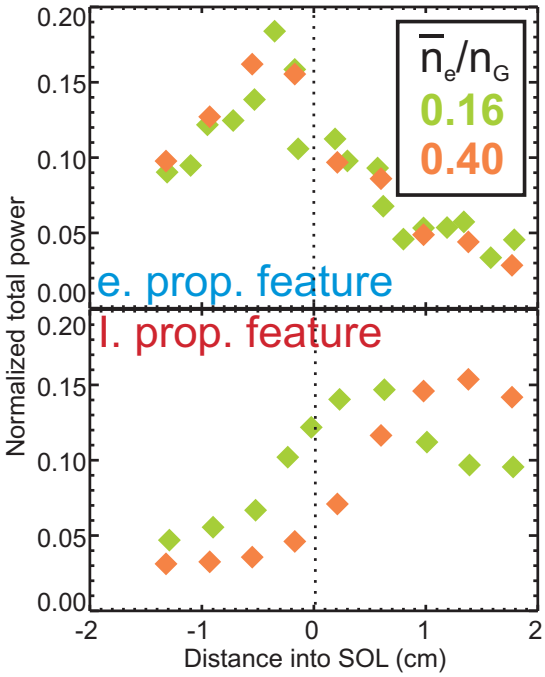

FIG. 4. Radial profile of the total intensity of the features in Fig.2 from two plasmas with extremes of the Greenwald fraction. The plot of the electron diamagnetic direction propagating feature in the low density case is the composite of two shots. The profiles were normalized to sum up to unity, so that trends can be compared.

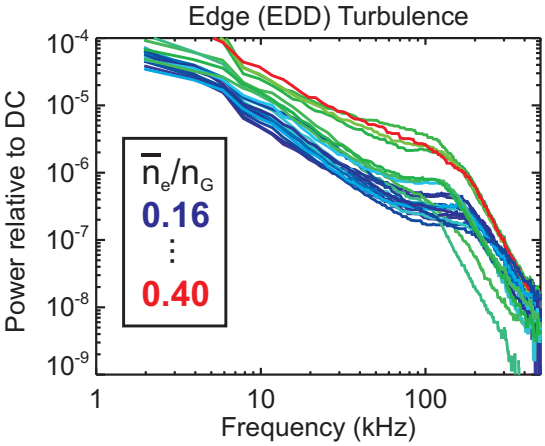

FIG. 5. (color online) Edge turbulence spectra normalized to average brightness values with a $k_{pol} > 0$ filter for $0.15 < \bar{n}_e/n_G < 0.45$. The curves are color coded for Greenwald fraction in a rainbow scheme going from low F_{Gr} (blue) to high (red). Lower F_{Gr} curves generally fall under the higher F_{Gr} ones.

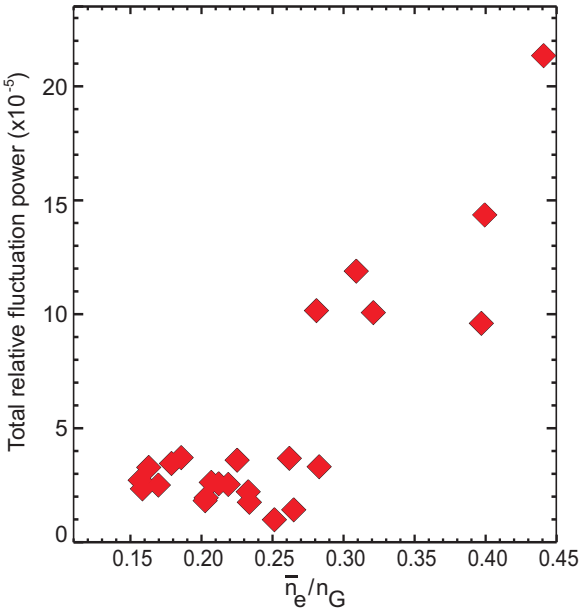

FIG. 6. Sum of the fluctuation power relative to the DC level above 50 kHz from the EDD turbulence.

is in fact a limit set by turbulent transport, but indicates as well that the key region for the turbulent transport is the edge, indeed the turbulence with positive k_{pol} in the edge. More will be said about the effect of the edge turbulence on SOL spectra and the far SOL density in Sec. IV once H-mode results are clarified. For now we continue interpreting the edge spectra.

All curves in Fig. 5 exhibit an unmistakable break in slope. In the wide literature of turbulence it is customary (though not necessarily correctly) to refer to such breaks in the slope of power spectra as the scale of energy injection [24]. The frequency values at which these breaks occur cover a wide range from 100kHz to just above 300kHz. Since, however, the k_{pol}-f spectra are well fitted by a constant propagation velocity, one can evaluate the spatial scales of the break in slope simply as

$$k_{pol} = \frac{2\pi f}{v_{EDD}},$$

a generous gain, considering that the time resolution of our system far exceeds its spatial resolution capabilities; and a useful transformation since the wavenumber is unaffected by the choice of the reference frame. The literature of theoretical treatment of edge turbulence on the other hand prefers $k_\perp \rho_s$ as a parameter, for its significance in the equations describing drift-wave turbulence [25] (ρ_s is the ion gyro-radius at the sound speed). The characteristic

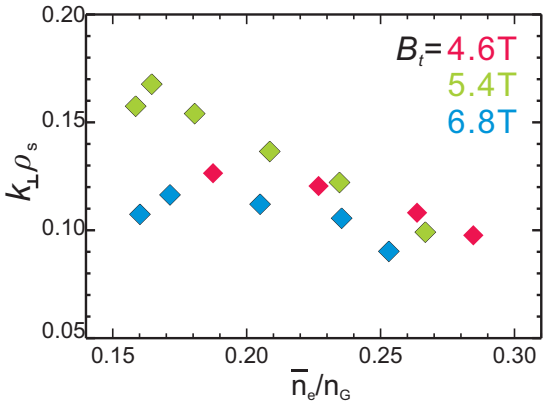

FIG. 7. Drift-normalized wavenumbers of the break in slope in the edge turbulence spectra from $q_{95} = 5$ discharges.

values found experimentally fall in the range $k_\perp \rho_s \in [0.09, 0.17]$ (cf. ref. [25] where this is the range both in $k_\perp \rho_s$ and α_d where both drift waves and interchange instabilities may be important). Further, we find that even after adjusting for the propagation speeds and normalizing the resulting break in slope wavenumber k^c_{pol} to the sound gyro-radius, a trend remains in the $k^c_{pol}\rho_s$ values. This trend is shown in Figure 7 with $k^c_{pol}\rho_s$ showing a slight decrease as F_{Gr} increases. These break in slope wavenumbers then lend themselves as division points for further inspection of the spectra: the reason why they might represent the scale of energy injection is that spectral transfer is expected to be different towards larger structures than towards smaller ones, and even if these critical wavenumbers cannot be identified as such, their importance remains as the spatial scale where factors of turbulence drive and dissipation change essentially.

One conspicuous feature of the power spectra above this point is that they all show a power-law decay $P(f) \propto f^{-\gamma}$, a tendency considered customary after the formulation of the Kolmogorov-scaling, but demonstrated here only above 200kHz. The decay exponents, or spectral indices, of the spectra from all experiments were determined by least-square fits, which provided values of $\gamma = 4.1 \pm 0.4$, in the range of regularly predicted theoretical values for both interchange and drift wave turbulence. Below the break in slope, on the other hand, a considerable variety of spectral shapes is seen, with the trends as a function of F_{Gr} shown in Fig. 8.

At low Greenwald fractions, we find that the spectrum has a slight, sometimes even a pronounced peak at the high frequency ($\sim$ 200kHz) end of the spectra. We return to discussing

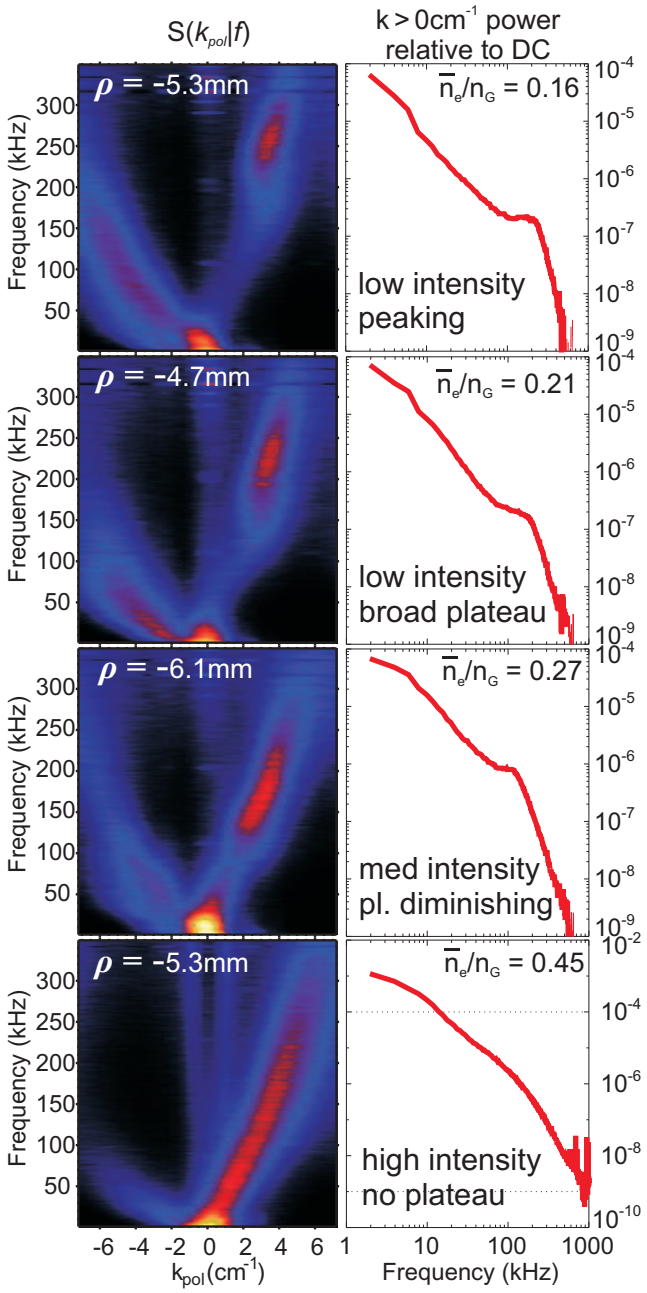

FIG. 8. Conditional wavenumber–frequency spectra from the edge region of L-mode plasmas, plotted for a wide range of Greenwald fractions. The corresponding turbulence spectra on the right show only the positive k_{pol} component in order to filter the data from any effects caused by the blobby SOL component which is subdominant in this region. The intensity of the turbulence goes up rapidly at $F_{Gr} \approx 0.25$

the significance of this point in the next subsection. As the Greenwald fraction increases, this feature becomes a plateau, eventually giving way to a fully developed turbulent spectrum, in which it is manifested as the break in slope. Accompanying these changes the overall turbulence intensity increases as noted above. Thus the positive k_{pol} turbulence in the the edge responds quite sensitively to changes in the Greenwald fraction, filling in more and more size scales with higher and higher intensities as the density increases. Given the observations [13] of increased particle transport with increased F_{Gr}, the new observations regarding the dependence of edge turbulence on F_{Gr} suggest a close connection to edge particle transport. The behavior of cross-field edge transport, on the other hand, shows even more dramatic changes as the plasma undergoes an L-to-H transition.

B. H-mode

Studies of the edge turbulence in the L-H transition were conducted in LSN discharges, with $\mathbf{B} \times \nabla \mathbf{B}$ in the direction favorable for transitions, ie toward the active X-point. Both Ohmic and ICRF heated H-modes were studied. In Ohmic H-modes, the transition was triggered by ramping the toroidal field down to $B_T = 2.8$T, subsequently raising the field back to a value that put $q_{95} > 3.3$ to facilitate access to the Enhanced D-Alpha H-mode [1, 26]. In order to exclude any effects having to do with changing values of the field, or the safety factor, we also studied ICRF heated H-modes with a fixed magnetic field of $B_T = 5.4$T and a heating power of $P_{RF} = 2.5$MW triggering the transition. As long as the safety factor value does not inhibit the onset of an EDA H-mode, the transition sequence is roughly the same in both Ohmic and ICRF heated H-modes: L-mode $\rightarrow$ ELMfree H-mode $\rightarrow$ EDA H-mode, so all three regimes are studied in each case. In no case were there discreet ELMs observed.

Differences in the turbulence and turbulent fluxes have been noted in a number of studies (see e.g. [27], [28], or the review [29] and the references within). The prominent changes found in the edge turbulence as the above sequence occurs are demonstrated in Fig. 9. The L-mode turbulence plotted in the figure has a $k^c_{pol}\rho_s = 0.13$. ELMfree H-modes exhibit a much reduced outward cross-field transport, both main species and impurity density increases roughly linearly with time in such plasmas, eventually leading to radiative collapse unless another H-mode regime is accessed. In this phase, the k-filtered spectrum reveals that the positive k_{pol} features decrease by over a factor of 10 in power. Filtering known sources of

noise brings back a faint $k_{pol} > 0$ feature at $f > 250$kHz with a poloidal propagation velocity of ~ 25km/s, approximately consistent with the results of ref. [23] (derived using Charge-Exchange-Recombination-Spectroscopy) where the E_r in the edge of ELMfree plasmas is found to be on the order of 100kV/m, yielding $v_E \approx 20$km/s. Due to the low intensity, however, no radial velocity profile has yet been assembled, therefore the match to CXRS results is still somewhat limited. As the transition from ELMfree to EDA H-mode occurs, the QCM appears on the positive k_{pol} side in the edge with $k_{pol}^{QCM}\rho_s = 0.11$, which is suggestive of a connection between the underlying instability of the QCM and the possible energy injection scale of the L-mode turbulence. A connection is further reinforced by the fact that spectral powers at frequencies and wavenumbers somewhat smaller than those of the QCM remain reduced compared to L-mode levels, perhaps pointing to inhibited spectral transfer, which may be the reason the QCM can grow strong. The QCM is known to be responsible for increased cross-field particle transport [17], and is now suggested as a further manifestation of the underlying drive of L-mode edge turbulence. One further argument for the edge turbulence, as opposed to the SOL turbulence being responsible for this transport is made by following the evolution of the SOL spectra through the transition. The negative k_{pol} (IDD propagating) spectra of the SOL turbulence (the blobs) *are invariant through these important changes* when normalized to the average brightness levels, as is evident from Fig. 10.

The above results have been reproduced for both the Ohmic and the ICRF heated H-mode discharges. No significant changes were found, adding to the correlation of strong cross-field particle flux and *edge* turbulence.

IV. DISCUSSION

Using fast (2 MHZ) 2D Gas-Puff-Imaging viewing the 4 cm radial region at the low-field-side of Alcator C-Mod, we examined the turbulence both in the edge and in the SOL. We distinguished two connected but distinctly different regions in L-mode plasmas: in the *edge* inside the LCFS, the dominant broadband turbulence propagates poloidally in the electron diamagnetic drift direction. In the far SOL the turbulent structures (blobs) move poloidally in the opposite direction, consistent with the $\mathbf{E} \times \mathbf{B}$ direction and magnitude there. We presented evidence that it is primarily the turbulence of the edge region that is closely linked

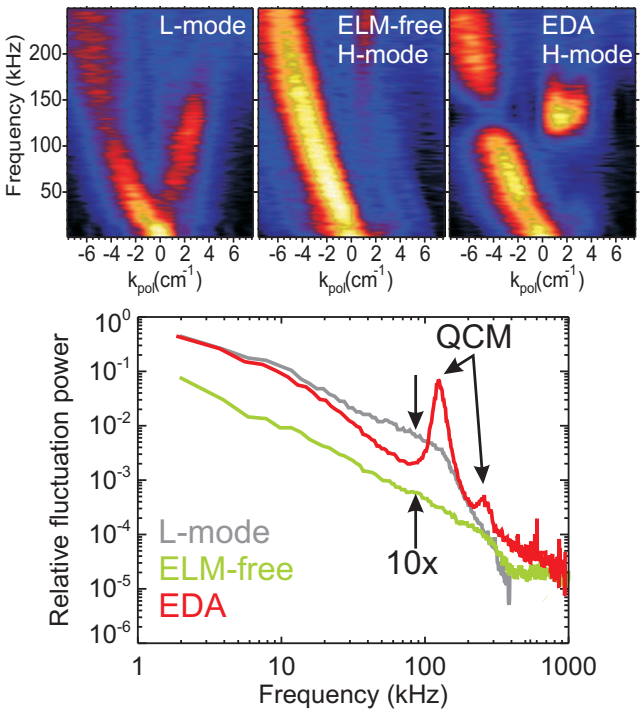

FIG. 9. Changes in the edge turbulence spectrum at the L-to-H transition. The top part of the figure shows conditional k-f spectra (normalized to every band in frequency), from the edge of an Ohmically heated plasma undergoing a transition in (from left to right) the L-mode, the ELMfree H-mode and the EDA H-mode phases. The single lobe in the ion diamagnetic drift direction is not getting stronger in the middle graph, the increased visibility is an artifact of the normalization, and so is the apparent dip in the same lobe at the frequency of the QCM. The bottom figure shows the k-filtered spectra from the three regimes, with a $\sim 10\times$ drop in power from L-mode to ELMfree, and the QCM appearing at the breaking point of the spectrum in EDA.

with cross-field particle transport in this region. Poloidal-wavenumber–frequency spectra from the edge are found to be well approximated by a linear dispersion relation allowing to express power spectra as a function of $k_{pol} = 2\pi f / v_{EDD}$, which is not subject to any Doppler-shifts. Results show a clear break in slope of power vs k_{pol} at k^c_{pol} with $k^c_{pol}\rho_s = 0.09 - 0.17$ over a range of magnetic fields and densities. Below this value, there is a clear dependence of the spectra upon Greenwald fraction, with the power of the turbulence increasing with $\bar{n}_e/n_G$, and the power at wavenumbers lower than the characteristic k^c_{pol} filling in as the edge becomes more turbulent and spectral transfer is enhanced. In ELMfree H-mode plasmas, this turbulence shows a dramatic drop in power and speeds up to $\sim$ 25km/s, approximately

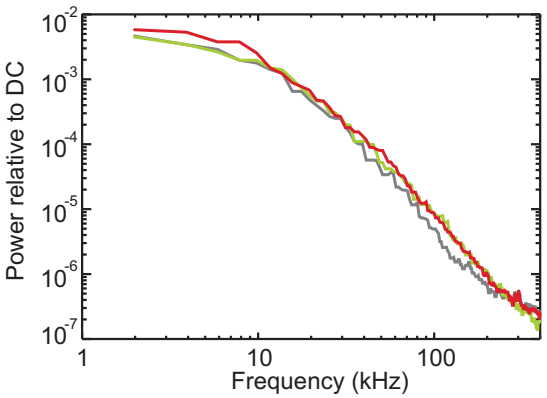

FIG. 10. The power spectrum of the SOL turbulence relative to the DC brightness level. The L-mode (green), ELM-free H-mode (black) and EDA H-mode (red) curves are spectra are essentially indistinguishable.

consistent with a concurrent increase in the E_r-well depth there. If the ELMfree H-mode evolves into an H-mode with a QCM, the QCM develops in this region with $k_{pol}^{QCM}\rho_s = 0.1$, suggesting a possible connection with the turbulence input scale seen in L-mode. The SOL turbulence on the other hand seems largely unaffected by even the changes brought about by the L-H transition, as shown in Fig. 10. This result merely underlines the importance of edge turbulence and is *not* inconsistent with previous findings from other tokamak experiments [27, 28], in which the frequency or intensity of blobs, or the particle flux was observed to drop in the L-H transition. It needs to be emphasized, however, that the spectra in Fig. 10 are normalized to the average brightness level, and therefore the one from the higher confinement plasma, ie lower SOL density does represent an *absolute* drop in either blob frequency or intensity. Previous studies have also shown that plasma in the far SOL is primarily the result of blobs born near the LCFS (see eg [6]), explaining how invariant normalized spectra can still represent different particle fluxes from the edge region[7]. The new observation also ties in well with previous results from Alcator C-Mod, especially in ref. [13] where density in the far SOL is shown to systematically fill in relative to the edge at Greenwald fractions $F_{Gr} \approx 0.3$, indicating an enhanced cross-field particle transport. Here we show the relative intensity of the *edge* turbulence increasing at a similar value of F_{Gr}.

In this paper we have concentrated on the propagation and the behavior of the edge turbulence, but the trend of the poloidal propagation velocities of the SOL turbulence with Greenwald fraction can also help strengthen our understanding. Figure 11 shows trends in

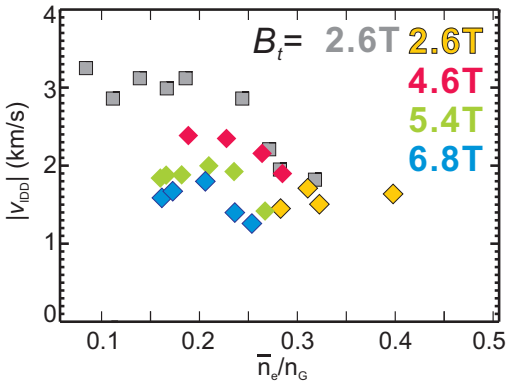

FIG. 11. Measured propagation velocities in the SOL in the ion diamagnetic drift direction against Greenwald fraction at different toroidal fields. The grey points at 2.6T are from the 2007 campaign, all others are from the present experiment.

the poloidal velocity of the SOL turbulence from the 2007 campaign together with recent results. At the Greenwald fraction where the edge turbulence starts to grow the phase velocities in the IDD direction decrease for each value of magnetic field. The trend supports our statement that the far SOL blob velocity is $\mathbf{E} \times \mathbf{B}$.

In view of ref. [14] the edge-SOL system is considered to exist at a critical α_{MHD}, normalized pressure gradient. If however the density increases, ∇T_e is expected to decrease unless completely different physics (like H-mode) enters. But $E_r \propto \nabla T_e$ in the SOL, therefore v_E is expected to decrease with density. Moreover there is also a clear decreasing tendency with toroidal field, qualitatively consistent with $v_E = E_r/B_T$.

Even though it is not possible to know from these measurements the exact physics of the underlying instability for blob generation, the picture that is starting to take shape from these findings and those of [14, 15] seems very similar to the one presented in [12], and is roughly the following. The edge density and temperature profiles are set by gradient limiting transport mechanisms. This manifests itself as the QCM in EDA regimes, and through spectral transfer from this instability to larger features, as broad-band turbulence in L-mode. This development towards larger features is hindered if: a) n_e/n_G is very small (peaked spectra), b) there is a strong edge flow as in ELM-free and EDA discharges. These features are wavelike, moving poloidally at a velocity set by their specific dispersion (v_D and v_E together), and their amplitude may become large enough to go beyond a critical gradient at which plasma is pushed across the field, at which point, instead of a wave motion (which

does not involve poloidal particle drift) separate blobs of plasma travel through the SOL following v_E of that region.

Of course this conjecture is not complete. Not only does it not identify the underlying instability, it also gives no explanation to the existence of the IDD propagating feature in ELMfree H-mode as deep as $\rho = -1.5$cm where the $v_E \approx 25$km/s. This point raises possibility of "contamination" of the measurements by the intrinsic, non-localized D_α emission or of systematic instrumental effects associated with GPI. We have examined the possibility that the IDD propagating features at $\rho \lesssim -1$cm are due to non-localized intrinsic emission or to toroidal spreading of the local gas puff, leading to emission along the line-of-sight from a $\rho > 0$. Neither possibility is quantitatively consistent with the observations. Thus at present, we have no satisfactory explanation for the existence of the IDD feature well inside the LCFS and coexisting with the EDD feature.

ACKNOWLEDGMENTS

The authors would like to thank Olaf Grulke and Stewart Zweben for the discussions and the insightful comments as well as the Alcator C-Mod team of students, scientists, engineers and technical staff for making the experiments possible. This work is supported by U.S. Department of Energy Cooperative Agreement No. DE-FC02-99ER54512

[1] J.W. Hughes, D.A. Mossessian, A.E. Hubbard, B. Labombard and E.S. Marmar Phys. Plasmas **9**, 3019 (2002)

[2] T.H. Osborne, R.J. Groebner, L.L. Lao, A.W. Leonard, R. Maingi, R.L. Miller, G.D. Porter, D.M. Thomas and R.E. Waltz, Plasma Phys. Control. Fusion **40**, 845 (1998)

[3] W. Suttrop, M. Kaufmann, H.J. de Blank, B. Brüsehaber, K. Lackner, V. Mertens, H. Murmann, J. Neuhauser, F. Ryter, H. Salzmann, J. Schweinzer, J. Stober, H. Zohm and the ASDEX Upgrade Team, Plasma Phys. Control. Fusion **39**, 2051 (1997)

[4] B. LaBombard, R.L. Boivin, M. Greenwald, J. Hughes, B. Lipschultz, D. Mossessian, C.S. Pitcher, J.L. Terry, and S.J. Zweben, Phys. Plasmas **8**, 2107 (2001)

[5] S. Zweben, Phys. Fluids **28**, 974 (1985)

[6] J.A. Boedo, D. Rudakov, R. Moyer, S. Krasheninnikov, D. Whyte, G. McKee, G. Tynan, M. Schaffer, P. Stangeby, P. West, S. Allen, T. Evans, R. Fonck, E. Hollmann, A. Leonard, A. Mahdavi, G. Porter, M. Tillack, G. Antar, Phys. Plasmas **8**, 4826, (2001)

[7] The spectra are normalized to average brightness and not SOL density, but the relative constancy of the temperature of this region in all regimes makes it possible to consider the two normalizations equivalent here.

[8] S.J. Zweben, R.J. Maqueda, D.P. Stotler, A. Keesee, J. Boedo, C.E. Bush, S.M. Kaye, B. LeBlanc,J.L. Lowrance, V.J. Mastrocola, R. Maingi, N. Nishino, G. Renda, D.W. Swain, J.B. Wilgen, N. Team, Nucl. Fusion **44**, 134, (2004)

[9] F. Sattin, M. Agostini, P. Scarin, N. Vianello, R. Cavazzana, L. Marrelli, G. Serianni, S.J. Zweben, R.J. Maqueda, Y. Yagi, H. Sakakita, H. Koguchi, S. Kiyama, Y. Hirano, J.L. Terry, Plasma Phys. Cont. Fus., **51**, 055013, (2009)

[10] R. Sánchez, B.Ph. van Milligen, D.E. Newman, and B.A. Carreras, Phys. Rev. Lett. **90**, 185005 (2003)

[11] M. Spolaore, V. Antoni, E. Spada, H. Bergsåker, R. Cavazzana, J.R. Drake, E. Martines, G. Regnoli, G. Serianni, and N. Vianello, Phys. Rev. Lett. **93**, 215003 (2004)

[12] I. Furno, B. Labit, M. Podestà, A. Fasoli, S.H. Müller, F.M. Poli, P. Ricci, C. Theiler, S. Brunner, A. Diallo and J. Graves, PRL **100**, 055004 (2008)

[13] B. LaBombard, Nucl. Fusion **45**, 1658-1675 (2005)

[14] B. LaBombard, J.W. Hughes, N. Smick, A. Graf, K. Marr, R. McDermott, M. Reinke, M. Greenwald, B. Lipschultz, J.L. Terry, D.G. Whyte, S.J. Zweben, and Alcator C-Mod Team, Phys. Plasmas **15**, 056106 (2008)

[15] J.W. Hughes, Nucl. Fusion **47** 1057 (2007)

[16] A.E. Hubbard, R.L. Boivin, R.S. Granetz, M. Greenwald, J.W. Hughes, I.H. Hutchinson, J. Irby, B. LaBombard, Y. Lin, E.S. Marmar, A. Mazurenko, D. Mossessian, E. Nelson-Melby, M. Porkolab, J.A. Snipes, J.L. Terry, S. Wolfe, and S. Wukitch, Phys. Plasmas **8**, 2033 (2001)

[17] J.L. Terry, N.P. Basse, I. Cziegler, M. Greenwald, O. Grulke, B. LaBombard, S.J. Zweben, E.M. Edlund, J.W. Hughes, L. Lin, Y. Lin, M. Porkolab, M. Sampsell, B. Veto and S.J. Wukitch, Nucl. Fusion **45**, 1321 (2005)

[18] M. Greenwald, Plasma Phys. Control. Fusion **44**, 27 (2002)

[19] L. C. Johnson and E. Hinnov, Quant. Spectrosc. Radiat. Transfer **13**, 333 (1973)

[20] J.W. Hughes, D.A. Mossessian, A.E. Hubbard, and E.S. Marmar, Rev. Sci. Instrum. **72**, 1107 (2001)

[21] M. Greenwald, J.L. Terry, S. Wolfe, S. Ejima, M. Bell, S. Kaye, G.H. Neilsen, Nucl. Fusion **28**, 2199 (1988)

[22] P. C. Stangeby, The Plasma Boundary of Magnetic Fusion Devices (Institute of Physics, Berkshire, 2000)

[23] R.M. McDermott, B. Lipschultz, J.W. Hughes, P.J. Catto, A.E. Hubbard, I.H. Hutchinson, R.S. Granetz, M. Greenwald, B. LaBombard, K. Marr, M.L. Reinke, J.E. Rice, D. Whyte, and Alcator C-Mod Team, Phys. Plasmas **16**, 056103 (2009)

[24] R.H. Kraichnan, Phys. Fluids **10** 1417 (1967)

[25] B.D. Scott, Phys. Plasmas **12**, 062314 (2005)

[26] M. Greenwald, Fusion Sci. Tech. **51**, 266 (2007)

[27] R.A. Moyer, J.W. Cuthbertson, T.E. Evans, G.D. Porter, J.G. Watkins, J Nucl. Mater., **241-243**, 633, (1997)

[28] A.E. White, S.J. Zweben, M.J. Burin, T.A. Carter, T.S. Hahm, J.A. Krommes, R.J. Maqueda, Phys. Plasmas, **13**, 7, (2006)

[29] J.A. Boedo, J Nucl. Mater. **390-391**, 29, (2009)

[30] B.A. Carreras, J. Nucl. Mater. **337-339**, 315 (2005)

[31] J. Myra and D. DIppolito, Phys. Plasmas **13**, 112502 (2006)

[32] I.H. Hutchinson, R. Boivin, F. Bombarda, P. Bonoli, S. Fairfax, C. Fiore, J. Goetz, S. Golovato, R. Granetz, M. Greenwald, S. Horne, A. Hubbard, J. Irby, B. LaBombard, B. Lipschultz, E. Marmar, G. McCracken, M. Porkolab, J. Rice, J. Snipes, Y. Takase, J.L. Terry, S. Wolfe, C. Christensen, D. Garnier, M. Graf, T. Hsu, T. Luke, M. May, A. Niemczewski, G. Tinios, J. Schachter, and J. Urbahn, Phys. Plasmas **1**, 1511 (1994)